Effects of Order on the Photophysical Properties of the Liquid Crystal Zinc Octakis(β-octoxyethyl)porphyrin

Brian A. Gregg, Marye Anne Fox,* and Allen J. Bard*

Department of Chemistry, University of Texas at Austin, Austin, Texas 78712 *(Received: August 8, 1988)*

Zinc octakis(β-octoxyethyl)porphyrin, a new, liquid crystalline organic semiconductor, forms more highly ordered thin films than its non liquid crystalline analogue zinc octaethylporphyrin. Films of these two porphyrins are employed to study the changes in the absorption, fluorescence emission, and fluorescence excitation spectra as the film order is increased from amorphous to crystalline. The blue-shift of the B band and the red-shift of the Q bands in the absorption spectra are described, for all but the most highly ordered films, in terms of the molecular exciton model. The quantum yield for fluorescence increases with increasing order and, in the most crystalline samples, becomes strongly wavelength-dependent, decreasing for shorter excitation wavelengths. This is evidence for possible ring-to-ring charge-transfer (RRCT) state formation in competition with internal conversion. Emission, excitation, and absorption spectra in the solid, liquid crystalline, and liquid phases show that the observed spectral shifts are a function of the organization, not merely the proximity, of the neighboring chromophores.

Introduction

The optoelectronic properties of thin films of organic semiconductors such as porphyrins and phthalocyanines have attracted attention for both practical[1] and theoretical[2,3] reasons. The mechanisms of electronic conduction, energy transfer, and radiationless deactivation of excited states in single crystals of organic semiconductors are still not well understood.[3] An understanding of these processes in the less well-ordered, but technologically more important, thin films is still in a primitive stage.

In the solid state, porphyrins, and many other organic semiconductors, behave as quasi-one-dimensional conductors;[3,4,5] their intermolecular overlap, and therefore their conductivity, is greatest in a direction perpendicular to the molecular planes. Because of the low dimensionality of the conducting pathway, crystal dislocations (see, for example, Figure 1) should have a greater effect on the optoelectronic properties of organic semiconductors than on three-dimensional semiconductors such as silicon. Such considerations led us to synthesize a series of discotic liquid crystalline porphyrins[6] possessing fluid phases in an effort to (a) investigate the effects of order on the photophysical and photoelectrochemical properties of these thin films and (b) grow large-area, well-ordered thin films for use in organic semiconductor devices.

A number of papers dealing with the photophysical properties of porphyrin thin films have appeared. Gouterman et al.[7a,b] have studied sublimed films of octaethylporphyrin (H_2OEP) and report that films thicker than ca. 100 Å have some tendency to crystallize spontaneously. These films showed increased impurity fluorescence that was attributed to a longer exciton diffusion length in the polycrystalline materials, as compared to the amorphous films. They also noticed a substantial quenching of the Soret band in the fluorescence excitation spectrum of the polycrystalline films,[7a] although this was later thought to be a reflection effect.[7b] These workers later showed[7c] that the emission intensity from both the host and the impurities was enhanced by sublimation onto a heated substrate, rather than one at room temperature.

A substantial effort has been devoted to the characterization of monolayer films of porphyrins, both as the pure porphyrins[8-10a,c,d] and as mixtures with surfactants.[10b] The optical properties of porphyrins in monolayers resemble those of the dimerized or aggregated species in solution.[8b,9,10a,b] A number of examples of conductivity measurements[8a,10c,d] and photoelectron transfer[8a,c] have also been reported. Kampas et al.[11] prepared both sublimed and spin-coated thin films of a large number of porphyrins for testing in photoelectrochemical (PEC) cells. The amorphous films obtained by spin-coating showed higher quantum efficiencies for photocurrent generation than the polycrystalline films obtained by sublimation, although this result might be explained by the possibility of a larger number of pinholes in the polycrystalline layers. Armstrong et al.[12] have carefully optimized the sublimation conditions for the deposition of a number of phthalocyanines and have correlated the changes in the absorption spectra with the type of crystals formed. They obtained the highest efficiencies in PEC cells for films consisting of large crystals that spanned the thickness of the layer. Working with liquid crystal phthalocyanines, Simon et al.[4b-d] have shown that the fluorescence is sharply decreased by heating the films to the liquid crystalline (LC) phase. The diffusion coefficient of the triplet excitons was also observed to increase in the LC phase relative to the solid. The rather short triplet exciton diffusion length (ca. 650 Å) was identified with the average length of the phthalocyanine columns.

With the availability of liquid crystalline porphyrins,[6] we are now able to exercise more control over the crystallinity of a thin film than was previously possible. This paper details how the

(1) See for example: (a) Loutfy, R. O.; Sharp, J. H.; Hsiao, C. K.; Ho, R. *J. Appl. Phys.* **1981**, *52*, 5218. (b) Loutfy, R. O.; Sharp, J. H. *J. Chem. Phys.* **1979**, *71*, 1211. (c) Leempoel, P.; Fan, F.-R. F.; Bard, A. J. *J. Phys. Chem.* **1983**, *87*, 2948. (d) Hackett, C. F. *J. Chem. Phys.* **1971**, *55*, 3178. (e) Meier, H.; Albrecht, W. *Ber. Bunsen-Ges. Phys. Chem.* **1969**, *73*, 86. (f) Musser, M. E.; Dahlberg, S. C. *Thin Solid Films* **1980**, *66*, 261. (g) Lecompte, C.; Boudin, C.; Ruaudel-Teixer, A.; Barraud, A.; Momenteau, M. *Thin Solid Films* **1985**, *133*, 103.

(2) Cave, R. J.; Siders, P.; Marcus, R. A. *J. Phys. Chem.* **1986**, *90*, 1436.

(3) (a) Pope, M.; Swenberg, C. E. *Electronic Processes in Organic Solids*; Oxford University Press: New York, 1982. (b) Simon, J.; Andre, J.-J. *Molecular Semiconductors*; Springer-Verlag: Berlin, 1985. (c) Gutman, F.; Lyons, L. E. *Organic Semiconductors, Part A*; Robert E. Krieger: Malabar, FL, 1981. (d) Gutmann, F.; Keyser, H.; Lyons, L. E. *Organic Semiconductors, Part B*; Robert E. Krieger: Malabar, FL, 1983.

(4) (a) Piechocki, C.; Simon, J.; Skoulios, A.; Guillon, D.; Weber, P. *J. Am. Chem. Soc.* **1982**, *104*, 5245. (b) Knoesel, R.; Piechocki, C.; Simon, J. *J. Photochem.* **1985**, *29*, 445. (c) Blanzat, B.; Barthou, C.; Tercier, N.; Andre, J.-J.; Simon, J. *J. Am. Chem. Soc.* **1987**, *109*, 6193. (d) Markovitsi, D.; Tran-Thi, T.-H.; Briois, V.; Simon, J.; Ohta, K. *J. Am. Chem. Soc.* **1988**, *110*, 2001.

(5) (a) Marks, T. J. *Science* **1985**, *227*, 881, and references therein. (b) Gaudiello, J. G.; Almeida, M.; Marks, T. J.; McCarthy, W. J.; Butler, J. C.; Kannewurf, C. R. *J. Phys. Chem.* **1986**, *90*, 4917. (c) Schoch, K. F., Jr.; Kundalkar, B. R.; Marks, T. J. *J. Am. Chem. Soc.* **1979**, *101*, 7071.

(6) (a) Gregg, B. A.; Fox, M. A.; Bard, A. J. *J. Chem. Soc., Chem. Commun.* **1987**, 1134. (b) Gregg, B. A.; Fox, M. A.; Bard, A. J. *J. Am. Chem. Soc.*, in press.

(7) (a) Bonham, J. S.; Gouterman, M.; Howell, D. B. *J. Lumin.* **1975**, *10*, 295. (b) Kampas, F. J.; Gouterman, M. *J. Lumin.* **1976**, *14*, 121. (c) Kampas, F. J.; Gouterman, M. *J. Lumin.* **1978**, *17*, 439.

(8) (a) Bardwell, J. A.; Bolton, J. R. *Photochem. Photobiol.* **1984**, *40*, 319. (b) Bardwell, J. A.; Bolton, J. R. *Photochem. Photobiol.* **1984**, *39*, 735. (c) Janzen, F. A.; Bolton, J. R. *J. Am. Chem. Soc.* **1979**, *101*, 6342.

(9) Zachariasse, K. A.; Whitten, D. G. *Chem. Phys. Lett.* **1973**, *22*, 527.

(10) (a) Miller, M.; Knoll, W.; Moewald, H.; Ruaudel-Teixer, A. *Thin Solid Films* **1985**, *133*, 83. (b) Bull, R. A.; Bulkowski, J. E. *J. Colloid Interface Sci.* **1983**, *92*, 1. (c) Jones, R.; Tredgold, R. H.; Hoorfar, A. *Thin Solid Films* **1985**, *123*, 307. (d) McArdle, C. B.; Ruaudel-Teixer, A. *Thin Solid Films* **1985**, *133*, 93.

(11) Kampas, F. J.; Yamashita, K.; Fajer, J. *Nature* **1980**, *284*, 40.

(12) (a) Klofta, T. J.; Danziger, J.; Lee, P.; Pankow, J.; Nebesny, K. W.; Armstrong, N. R. *J. Phys. Chem.* **1987**, *91*, 5646. (b) Klofta, T. J.; Sims, T. D.; Pankow, J. W.; Danziger, J.; Nebesny, K. W.; Armstrong, N. R. *J. Phys. Chem.* **1987**, *91*, 5651.

0022-3654/89/2093-4227$01.50/0

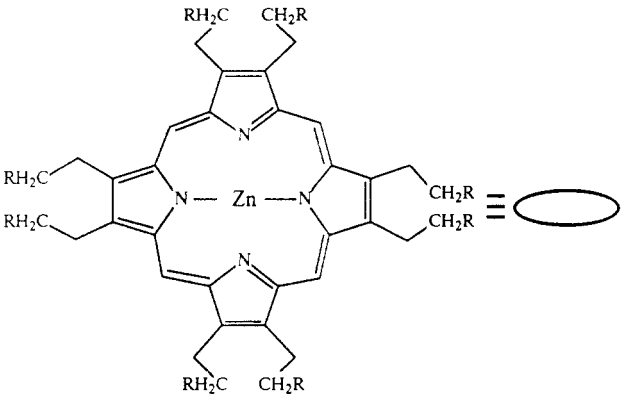

a

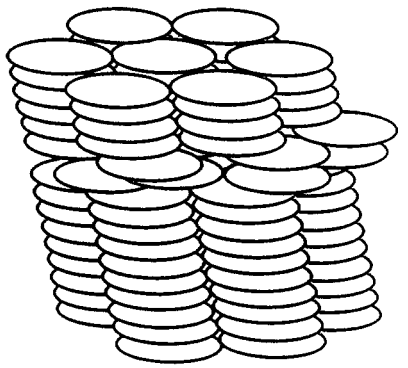

b

Figure 1. (a) Zinc octaethylporphyrin (ZnOEP) and zinc octakis(β-octoxyethyl)porphyrin (ZnOOEP). (b) A schematic diagram of a columnar discotic phase with crystal dislocations.

photophysical properties of the liquid crystal zinc octakis(β-octoxyethyl)porphyrin[6b] (ZnOOEP, Figure 1), and its non liquid crystalline analogue zinc octaethylporphyrin (ZnOEP, Figure 1), change as a function of the degree of film order and, for ZnOOEP, as a function of phase. The present work contains the following points: (1) a description of the photophysical changes in a system of a single chromophore (octaalkylporphyrin) whose degree of order can be almost continually varied between amorphous and crystalline; (2) an explanation for why the porphyrin Q and B absorption bands are shifted in opposite directions with increasing order; (3) a demonstration that the absorption band at ca. 486 nm is probably not the B^- band; (4) a demonstration that the quantum yield for fluorescence, Φ_f, increases with order; (5) a demonstration that Φ_f becomes wavelength-dependent above a certain degree of order; (6) a comparison of the photophysical properties of free-floating crystals with those of the thin films and the dissolved species; and (7) a measurement of the photophysical changes as the phase changes from the solid to the liquid crystal to the liquid. To the best of our knowledge, a number of these points are quite novel.

It should be emphasized that ZnOOEP is a solid at room temperature. Its liquid crystalline phase (from 107 to 162 °C) and its liquid phase are useful for attaining an ordered state (i.e., by slow cooling from the isotropic liquid, through the liquid crystalline phase, to the solid). However, the measurements reported here, unless otherwise noted, were taken at room temperature.

Experimental Section

Materials. Zinc octakis(β-octoxyethyl)porphyrin, ZnOOEP, and zinc octaethanolporphyrin (zinc octakis(β-hydroxyethyl)-porphyrin) were prepared and purified as described previously.[6b] Zinc octaethylporphyrin, ZnOEP, was purchased as the free base from Midcentury Chemicals, metalated by a standard procedure,[6b] and recrystallized once from $CHCl_3$/methanol and once from THF/methanol. Xylene and THF were reagent grade and were distilled before use. Pyridine, 1,2-dichloroethane (DCE), 1,3,5-triethylbenzene (TEB), and dodecane were reagent grade and were used as received.

Instrumentation. The spin coater was a Pine Instruments Co. analytical rotator. The glass plates were attached to the spinner with double-stick tape, and one or two drops of coating solution was applied at the appropriate spin rate. All films were smooth to the eye and appeared uniform under 100× magnification.

Absorption spectra were measured on a Hewlett-Packard 8451A single-beam spectrophotometer with unpolarized light. The references used were an uncoated glass plate for the thin films, air for the capillary-filled cells, and a pure solvent-filled cell for the solution cells.

The optical textures of the films were observed in a Leitz Laborlux D polarizing microscope equipped with a hot stage. The hot stage was removed from the microscope and mounted in an SLM Aminco SPF 500 spectrofluorometer for the temperature-dependent fluorescence measurements. In this instrument, the emission is monitored at 90° to the excitation beam. The front-face cell holder held the sample surface at 65° to the incident light, unless otherwise noted. The excitation bandwidth was 2 nm; the emission bandwidth was either 1 or 2 nm. Scattering problems inherent in front-face operation made it impossible, even with filters, to excite into the Q bands while monitoring the emission from the Q bands. Therefore, all emission spectra employed excitation in the Soret (or B) region (<420 nm) and a 530-nm-long pass filter inserted before the emission monochromator. For the excitation spectra, the emission was monitored at 650 nm after passing through a 630-nm-long pass filter. Still, it was found necessary to subtract a blank excitation spectrum with use of an uncoated glass plate or a cell filled with pure solvent as the blank. All spectra were run in the ratio mode, which corrects for variation in lamp intensity with wavelength and time. Emission spectra were corrected for the photomultiplier response with the correction factor curve supplied with the instrument. Excitation spectra were corrected by dividing out the lamp profile that was obtained by use of a Rhodamine B solution as a quantum counter for the range λ = 350–500 nm and by use of a silicon photodiode (Oriel) for λ = 400–650 nm.

Films and Cells. The glass plates used were either 1.6-mm-thick indium tin oxide (ITO) coated float glass from Delta Technologies or 1-mm-thick microscope slides. The glass was cleaned by sonication in a KOH/2-propanol solution followed by copious rinsing with deionized water. It was then rinsed sequentially with 95% ethanol, distilled acetone, and reagent-grade 2-propanol before being dried at 120 °C in air.

If a glass plate coated with ZnOOEP was heated to above the liquid crystal to isotropic liquid transition temperature, 162 °C, the ZnOOEP would begin to coalesce into droplets, leaving patches of uncovered glass. This greatly complicated the comparison of the "ordered" to the "as-spun" porphyrin layers. The following treatment of the ITO plates greatly reduced, but did not eliminate completely, the tendency to coalesce: a very dilute solution of zinc octaethanolporphyrin in pyridine was spun onto a dry ITO plate, which was then baked at 180 °C for 5 min. The plate was then exposed to a warm solution of hexamethyldisilazane (Aldrich) in toluene for 30 min, rinsed with toluene, and dried at 120 °C. All thin films described in the text used ITO substrates that had been treated in this manner. Surprisingly, this procedure did not work for the microscope slides. To prevent coalescence, these could be precoated with a thin layer of poly(vinylpyridine) (Polysciences). However, this introduced another peak into the absorption and excitation spectra because of pyridine complexation with the zinc porphyrin. Therefore, these plates were used only for control experiments.

The best solution for spin-coating ZnOOEP was xylene containing 5% pyridine. There was no evidence for pyridine com-

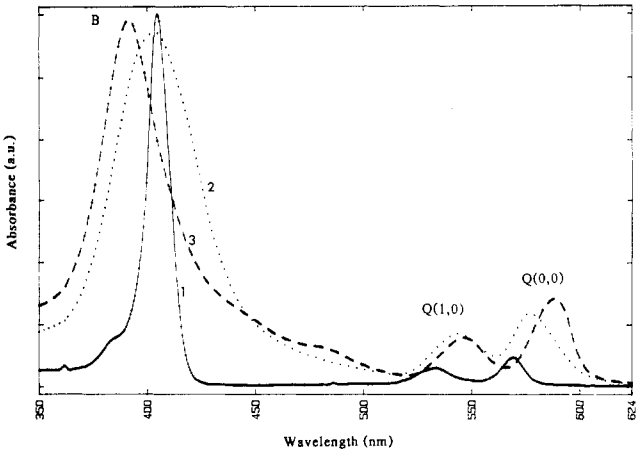

Figure 2. Absorption spectra: (1) ZnOOEP in triethylbenzene solution, 100-μm cell, —; (2) ZnOEP thin film spin-coated from DCE/pyridine, ···, (3) ZnOEP thin film spin-coated from THF, --. Absorbance units are arbitrary; see Table I for spectral data.

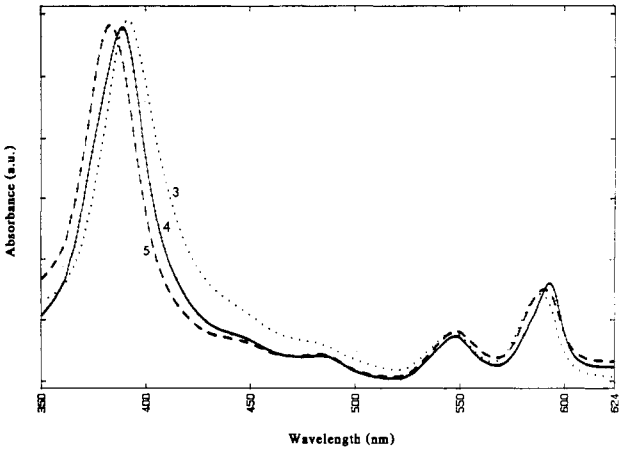

Figure 3. Absorption spectra: (3) same as 3 in Figure 2, ···; (4) ZnOOEP thin film as spun, —; (5) film 4 after heating to the isotropic liquid and cooling slowly to room temperature, --. Absorbance units are arbitrary; see Table I for spectral data.

plexation in the thin films, and their spectral properties were unaffected by being held in a vacuum for 24 h or by the substitution of 1-butanol for pyridine in the coating solution. Spin-coating from pure xylene resulted in nonuniform films. The most highly ordered (see text) films of ZnOEP were obtained by spin-coating from a pure THF solution. The degree of order of ZnOEP films could be varied over a substantial range by the choice of solvent (this was not the case for the liquid crystal porphyrin), and the least ordered, but still continuous, films were obtained by spinning from a DCE/pyridine solution.

Several thin cells were made for optical measurements on dissolved and/or crystallized porphyrins. These consisted of two 1.5 cm × 2.5 cm pieces of microscope slides, offset and separated by Teflon tape spacers (ca. 100 μm thick) and sealed with epoxy cement. The pure ZnOOEP was capillary-filled into some even thinner cells that were made by spin-coating a spacer solution of poly(ethylene-*co*-vinyl acetate) (Scientific Polymer Products) onto a masked ITO plate. Removal of the Teflon tape mask left two strips of polymer that would adhere to another ITO plate, if assembled while still tacky. These cells could be made in a thickness range of 0.8–8 μm (as measured by the optical absorption of the porphyrin-containing cells). They were also sealed with epoxy cement. Some cells were made with only a single polymer strip spacer (wedge cells) so that the thickness varied from 0 to ca. 8 μm across the cell.

Although data are presented here for only a few specific thin films, these results have been qualitatively reproduced in over 100 samples.

Results and Discussion

Absorption Spectra of Spin-Coated Films. The absorption and emission properties of porphyrins have recently been reviewed.[13] All octaalkylporphyrins with a given central metal have practically identical spectral properties; the length of the alkyl chains or the substituents past the α-position have essentially no effect on the photophysics.[13] Thus, it is not surprising that the two porphyrins studied in this work, ZnOEP and ZnOOEP, are spectroscopically indistinguishable in dilute solution.

Figure 2, curve 1, shows the absorption spectrum of ZnOOEP in 1,3,5-triethylbenzene (TEB) solution. The three major absorption bands, in order of increasing energy, are termed the Q(0, 0), Q(1, 0), and the B, or Soret, bands. The Q(0, 0) band is the transition to the first excited singlet state (S_1), and the Q(1, 0) has one quantum of vibrational energy in S_1, while the B band is the transition to the second singlet (S_2).[13]

The absorption spectra of ZnOEP films, which depend on the degree of order in the films, depend upon the conditions used in the spin-coating. Curves 2 and 3, Figure 2, show the absorption spectra of thin solid films of ZnOEP spin-coated from dichloroethylene/pyridine and tetrahydrofuran (THF), respectively. As will become apparent from the later results, curve 3 represents a much more highly ordered film than curve 2. With the appropriate choice of spin-coating conditions, a range of films with the spectra intermediate between curves 2 and 3 has been obtained; curves 2 and 3 represent the extremes that we have been able to achieve. All of the absorption bands have been broadened in the solid state relative to solution, and the Q bands have been red-shifted while the B band is blue-shifted. In curve 3, the absorption bands have become narrower relative to 2, the spectral shifts have become greater, and the intensity of Q(0, 0) has increased relative to Q(1, 0). Also, two weak bands on the low-energy tail of the B band have appeared.

The spectral properties of the liquid crystal films of ZnOOEP were not changed by changing the solvents used for spin-coating. In Figure 3, curve 4 shows the absorption spectrum of a thin film of ZnOOEP spin-coated from xylene/pyridine. All solutions used for spin-coating gave a film with essentially the same spectrum as curve 4. Curve 3 from Figure 2 is reproduced for comparison. Compared to ZnOEP, the bands of the liquid crystal, ZnOOEP, show a further sharpening and spectral shift relative to curve 3 and a further increase of Q(0, 0) relative to Q(1, 0). The two weak bands around 448 and 486 nm are somewhat more distinct. The base line is slightly skewed because of reflection effects. We can explain the lack of solvent dependence in spin-coated films of ZnOOEP by noting that the long alkyl side chains of ZnOOEP give it a greater conformational mobility than ZnOEP. As the solvent evaporates during the spin-coating, ZnOOEP is better able to find conformational energy minima compared to the less mobile ZnOEP. This is analogous to a sublimation onto a hot versus a cold substrate: the hot substrate imparts a greater conformational mobility to the molecules than does the cold substrate, resulting in greater crystallinity of the sublimed film.

Curve 5 shows the spectrum of the same thin film as curve 4 after being briefly heated to above its isotropic transition temperature, 162 °C, and slowly cooled. A continuation of the same pattern of spectral changes is observed, except that now the Q(0, 0) band has become slightly weaker and broader and is blue-shifted relative to curve 4. Table I summarizes the spectral data from Figures 2 and 3.

When viewed in a microscope between crossed polarizers, films 2–4 transmit no light; that is, they show no order on a scale longer than the wavelength of visible light. Film 5 is clearly polycrystalline with crystallites on the order of 1 μm in diameter (as measured in the microscope). The capillary-filled cells (discussed in text below) contain crystallites that are up to several millimeters in diameter.

Spectral shifts such as those shown here are similar to those seen in porphyrin[14-17] or phthalocyanine[18-20] dimers or oligomers

(13) Gouterman, M. In *The Porphyrins*; Dolphin, D., Ed.; Academic: New York, 1978; Vol. 3.

TABLE I: Spectral Data

sample	band	λ_{max}, nm	A_λ[a]	fwhm,[b] nm	Stokes shift,[c] nm	N[d]	I[e]	$\Phi_{f,rel}$[f]
(1) ZnOOEP in TEB soln	B	406	0.207	12				
	Q(1, 0)	534	0.011	20	2 ± 1	1.00	281.3	1.00
	Q(0, 0)	570	0.016	13				
(2) ZnOEP thin film	B	404	0.133	47				
from DCE/pyridine	Q(1, 0)	544	0.020	ca. 30	12 ± 2	1.44	10.1	0.06 ± 0.02
	Q(0, 0)	576	0.027	25				
(3) ZnOEP thin film	B	392	0.271	38				
from THF	Q(1, 0)	548	0.032	26	5 ± 1	0.81	66.8	0.22 ± 0.04
	Q(0, 0)	588	0.061	20				
(4) ZnOOEP thin film,	B	388	0.276	33				
as spun	Q(1, 0)	548	0.032	23	3 ± 1	0.81	383.8	1.11 ± 0.21
	Q(0, 0)	592	0.070	17				
(5) ZnOOEP thin film,	B	384	0.261	31				
ordered	Q(1, 0)	548	0.033	26	4 ± 1	0.84	281.0	0.98 ± 0.16
	Q(0, 0)	590	0.059	21				
(6) ZnOOEP in	B	404	0.060	9				
dodecane soln	Q(1, 0)	532	0.002	18	2 ± 2	1.00	348.5	1.00
	Q(0, 0)	568	0.004	11				
(7) ZnOOEP crystallized	B	392	0.086	ca. 75				
from dodecane soln	Q(1, 0)	548	0.021	26	2 ± 2	0.76	314.7	1.03 ± 0.17[g]
	Q(0, 0)	594	0.034	20				
(8) ZnOOEP in capillary-	B	382	2.09	ca. 46				
filled cell	Q(1, 0)	546	0.285	28	8 ± 2			
	Q(0, 0)	586	0.354	22				

[a] Absorbance at λ_{max} (absorbance units). [b] Full width at half-maximum of absorption peaks. [c] Difference between the Q(0, 0) absorption and emission peaks. [d] N, defined by eq 3, is the amount of excitation light absorbed by the reference relative to the sample. Sample 1 is used as the reference for films 1–5 (emission bandwidth 1 nm). Sample 6 is used as the reference for films 6 and 7 (emission bandwidth 2 nm). [e] Integral of the corrected emission intensity. [f] Relative fluorescence quantum yield. $\Phi_{f,rel} = I_s N/I_r$ where I_s and I_r are the integrated emission intensities of the sample and reference, respectively, N is defined by eq 3, and the same references are used as for N. [g] Multiplied by 1.5 ± 0.2 to correct for B band quenching, see text.

and in thin films[7,12] and monolayers[8b,9,10a,b] For example, in the face-to-face porphyrin dimers of Chang,[14] Collman et al.,[15] and Leighton et al.,[16] the B band is blue-shifted and the Q bands are red-shifted compared with the monomeric porphyrins; the shifts increase with decreasing interplanar spacing. The shifts are commonly described in terms of the molecular exciton model[21] for excited-state resonance interactions in weakly coupled electronic systems. The coupling splits the absorption bands into a high-energy, E^+, and a low-energy, E^-, component, one of which is usually forbidden. The energy of the absorption peak in the aggregate, $E^\pm$, is related to its energy in the monomer, E^0, by

$$E^\pm = E^0 + D \pm V \qquad (1)$$

where D is analogous to a solvent shift and reflects the change in environment on going from monomer to multimer. This is commonly thought to cause a red shift (i.e., D is negative), although apparently no theoretical calculation of its value has been given.[21d] V is the exciton splitting term that for a linear, cofacial array of N units tilted at an angle of α from the array axis, is given by[21e]

$$V \approx 2\left|\left(\frac{N-1}{N}\right)\frac{M^2}{R^3}(1 - 3\cos^2\alpha)\right| \qquad (2)$$

where M is the monomer transition dipole moment and R is the center-to-center distance between the macrocycle units. For a cofacial geometry, the lower energy exciton component, E^-, is symmetry forbidden[21] and all oscillator strength is contained in the E^+ component.

Thus, the increasing blue-shift of the strongly allowed (large M) B^+ band with increasing order (curves 2–5 in Figures 2 and 3) can be explained by (1) a decreasing interchromophore spacing (R), (2) an increasing number of interacting units (N), and (3) a decreasing tilt angle of the porphyrins in the column (increasing α). From our data, we are not able to judge directly the relative importance of these factors, although, from eq 2, V is much more strongly dependent on R than on N or α.

From the data in Table I, one can estimate the relative transition dipole moments[14a,c] of the B and Q(0, 0) bands as $M_B^2/M_Q^2 \approx 20$. Thus, from eq 2, the exciton displacement (V_Q^+) of the Q bands toward higher energy is ca. 20 times smaller than that of the B band (V_B^+). Thus, the red-shift of the Q bands relative to the solution species must be governed primarily by the "solvent shift" parameter, D_Q. For curve 4, the red-shift of the Q(0, 0) band is $E_Q^+ - E_Q^0 = V_Q^+ + D_Q \approx 650\ cm^{-1}$. The slight blue-shift of Q(0, 0) oberved with further ordering (curve 5) may indicate that, at this degree of order, V_Q^+ begins to dominate D_Q in eq 1.

Several workers have assumed that the low-energy shoulder on the B^+ band, in our case appearing around 486 nm, represents the forbidden B^- transition and have used its value, with eq 1, to compute the exciton splitting: $2V = E_B^+ - E_B^-$. From eq 1, the position of the B^+ band, E_B^+, is related to the sum of the blue-shift caused by V_B^+ and the red-shift caused by D_B. For E_B^-, both V_B^- and D_B give a red-shift; that is, the total red-shift of B^- relative to the monomer should always be greater than the blue-shift of B^+. However, as can be seen from curves 3–5 in Figure 3, the 486-nm band does not shift appreciably while B^+ shifts 8 nm to the blue. Therefore, we believe that neither the 486-nm band nor the 448-nm band (which has rarely been resolved) can be at-

(14) (a) Chang, C. K. *J. Heterocycl. Chem.* **1977**, *14*, 1285. (b) Chang, C. K. *Adv. Chem. Ser.* **1979**, *No. 173*, 162. (c) The ratio of the transition dipole moments is $(M_B^2/M_{Q(0,0)}^2) \approx (\epsilon_{maxB}/\epsilon_{maxQ})(fwhm_B/fwhm_Q)(\lambda_{maxQ}/\lambda_{maxB}) \approx (3.2 \times 10^5/2.0 \times 10^4)(^{12}/_{13})(^{370}/_{406}) \approx 20$ where the extinction coefficients have been taken from: Buchler, J. W. In *Porphyrins and Metalloporphyrins*; Smith, K. M., Ed.; Elsevier: Amsterdam, 1975.

(15) Collman, J. P.; Anson, F. C.; Barnes, C. E.; Bencosme, C. S.; Geiger, T.; Evitt, E. R.; Kreh, R. P.; Meier, K.; Pettman, R. B. *J. Am. Chem. Soc.* **1983**, *105*, 2694, and references therein.

(16) Leighton, P.; Cowan, J. A.; Abraham, R. J.; Sanders, J. K. M. *J. Org. Chem.* **1988**, *53*, 733.

(17) Boxer, S. G. *Biochim. Biophys. Acta* **1983**, *726*, 265, and references therein.

(18) (a) Ciliberto, E.; Doris, K. A.; Pietro, W. J.; Reisner, G. M.; Ellis, D. E.; Fragala, I.; Herbstein, F. H.; Ratner, M. A.; Marks, T. J. *J. Am. Chem. Soc.* **1984**, *106*, 7748. (b) Pietro, W. J.; Ellis, D. E.; Marks, T. J.; Ratner, M. A. *Mol. Cryst. Liq. Cryst.* **1984**, *105*, 273.

(19) Kobayashi, N.; Lever, A. B. P. *J. Am. Chem. Soc.* **1987**, *109*, 7433.

(20) Fujiki, M.; Tabei, H.; Kurihara, T. *J. Phys. Chem.* **1988**, *92*, 1281.

(21) (a) Davydov, A. S. *Theory of Molecular Excitons*; Plenum Press: New York, 1971; translated by Dresner, S. B. (b) Kasha, M.; Rawls, H. R.; El-Bayoumi, M. A. *Pure Appl. Chem.* **1965**, *11*, 371. (c) Gouterman, M.; Holten, D.; Lieberman, E. *Chem. Phys.* **1977**, *25*, 139. (d) Yan, X.; Holten, D. *J. Phys. Chem.* **1988**, *92*, 409. (e) Kasha, M. In *Spectroscopy of the Excited State*; Di Bartolo, B., Ed.; Plenum Press: New York, 1976.

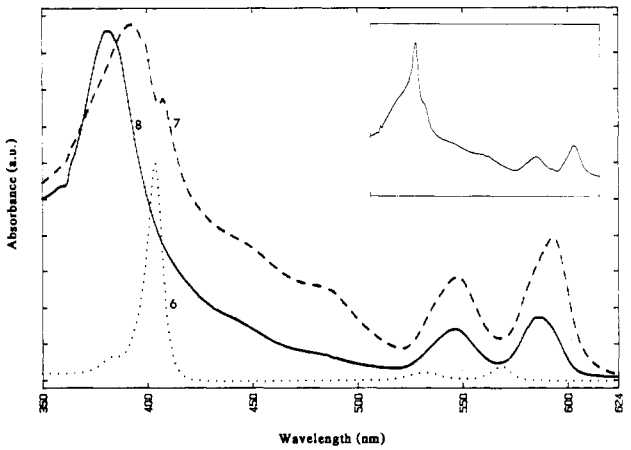

Figure 4. Absorption spectra: (6) ZnOOEP in dodecane solution, ···; (7) ZnOOEP crystallized from dodecane in a 100-μm cell minus spectrum 6, -- (inset, the spectrum of the cell before subtraction); (8) ZnOOEP capillary-filled into a 1.0-μm cell, —. Absorbance units are arbitrary; see Table I for spectral data.

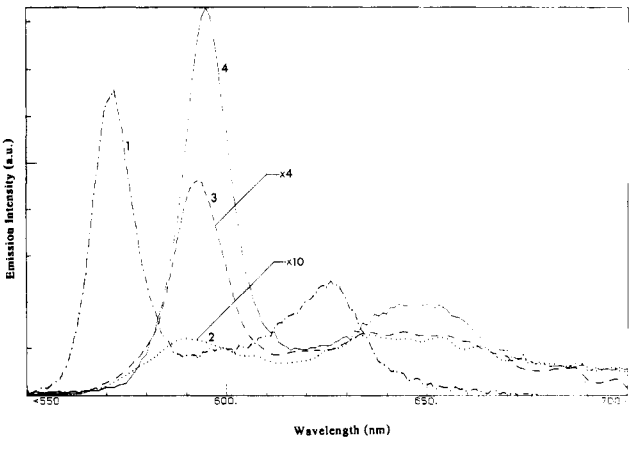

Figure 5. Corrected emission spectra. Numbers correspond to the samples shown in Figures 2 and 3. The samples were excited at the peak of the B band. Spectra are normalized to the absorbance of sample 1 through multiplication by the factor N (see Table I and text). Curves 2 and 3 are further multiplied by the factors shown.

tributed to B^-. This suggests that these bands are unrelated to the monomer Q and B transitions.

Broadening of the absorption bands in the solid state relative to solution is caused by both the same excitonic interactions that cause the splitting of the bands and by the inhomogeneity associated with the irregular orientation of neighboring molecules.[22] Thus, as the degree of order increases, the peaks become narrower. In the partially oriented liquid crystal, sample 5, the full width at half-maximum (fwhm) of the Soret band is the same as that observed for the face-to-face zinc porphyrin dimer described by Leighton et al.,[16] suggesting that its local environment is quite well-ordered.

The pattern of spectral shifts that emerges in the progression from curve 2 to 4 (and, in most respects, curve 5) in Figures 2 and 3 can be summarized as follows: the B band is progressively blue-shifted and narrowed; the bands at ca. 448 and 486 nm become more distinct; the Q bands are red-shifted; and Q(0, 0) is enhanced relative to Q(1, 0). From this consistent pattern, and from the fluorescence data given below, we conclude that these spectral shifts are an indication of the increasing degree of order along this progression.

Absorption Spectra of Crystallized and Capillary-Filled ZnOOEP. We wished to compare the photophysical properties of ZnOOEP crystallized from solution to its properties in solution and in the solid films. Thus, we recrystallized ZnOOEP from dodecane inside a 100-μm-thick glass cell by filling the cell with a hot dodecane solution of ZnOOEP and cooling to room temperature. An absorption spectrum of the cell consisted of ZnOOEP both in solution and in the crystalline state (inset, Figure 4). Subtraction of a normalized spectrum of ZnOOEP in dodecane, curve 6 in Figure 4, gives, approximately, the spectrum of crystalline ZnOOEP, curve 7. Qualitatively, the spectrum resembles those of the ZnOOEP thin films, curves 3 and 4; however, the B band is now extremely broad and weakened relative to the Q bands.

The spectrum of neat ZnOOEP capillary-filled into a ca. 1.0-μm-thick cell, curve 8, is also shown in Figure 4. Capillary-filling results in a polycrystalline film of the porphyrin containing crystals up to several millimeters in diameter (cf. Figure 4 in ref 6b). The spectrum of sample 8 is similar to that of the ordered film, curve 5, except that the B band is substantially broadened, the Q(0, 0) band is weaker, broader, and blue-shifted, and the Stokes shift (see text below) is increased relative to sample 5. Thus, several of the trends seen in the progression of films 2–4 have been reversed in this, the most highly ordered, sample. Sample 5 continues the trends seen in films 2–4 except that the Q(0, 0) band is slightly weakened and blue-shifted. Thus, the appearance of macroscopic crystallinity coincides with deviations from the pattern discussed above for the spin-coated films. It is not clear whether simple (weak-coupling) exciton theory can be applied to such systems. Also, as shown below, the fluorescence properties of the crystalline samples are markedly different from those of the less highly ordered films.

Emission Spectra. Figure 5 shows the emission spectra of the same thin films as in Figures 2 and 3. The emission spectrum of ZnOOEP in TEB solution, curve 1, was taken in a 100-μm-thick cell with the same front-face apparatus and conditions as for the thin films. A rough measure of the relative quantum yield of emission, $\Phi_{f,rel}$, of the thin films relative to the known quantum yield of these porphyrins in solution ($\Phi_f \approx 0.04$)[23] was then obtained by comparing the integrated emission intensities of the thin films to that of sample 1.

The emission spectra shown in Figure 5 are corrected for the instrumental response and are normalized at the B band to the absorbance of sample 1. Since the peak absorbances of these films (and of those to be discussed below) are typically >0.05, the ratio of the amount of light absorbed by a reference to that absorbed by a sample is given by the Lambert's law expression[24]

$$N = (1 - 10^{-A_{\lambda,r}})/(1 - 10^{-A_{\lambda,s}}) \quad (3)$$

where $A_{\lambda,r}$ and $A_{\lambda,s}$ are the measured absorbances at wavelength λ of the reference and sample spectra, respectively. N is needed to quantitatively compare the emission from different films or the absorption spectrum with the corresponding excitation spectrum. The values of N are listed in Table I with sample 1 used as the reference for the first five curves and sample 6 used as the reference for curves 6 and 7. All samples were excited at the peak of the B band. Table I also includes the Stokes shifts, the relative integrated emission intensities, and the relative quantum yields of fluorescence of the thin films.

The fluorescence emission of a porphyrin dimer, or solid film, is usually assumed[14,17] to be quenched relative to that of the monomer. Although quenching is a common result of interchromophore interactions,[7,8b,10a,19] there have been several reported systems where a dimer is either unquenched[17,21c] or actually emits more strongly[17] than the constituent monomers. In the solid state, for example, Φ_f for naphthalene single crystals is equal to its Φ_f in solution,[3a] while for anthracene single crystals Φ_f is increased relative to that in solution.[3a,25,26] Quenching seems to be the rule

(22) See for example: Suto, S.; Uchida, W.; Yashima, M.; Goto, T. *Phys. Rev. B: Condens. Matter* **1987**, *35*, 4393.

(23) Darwent, J. R.; Douglas, P.; Harriman, A.; Porter, G.; Richoux, M.-C. *Coord. Chem. Rev.* **1982**, *44*, 83.

(24) Parker, C. A. *Photoluminescence of Solutions*; Elsevier: Amsterdam, 1968.

(25) Wright, G. T. *Proc. Phys. Soc., London, Sect. B* **1955**, *68*, 241.

for any system involving a flexible linkage between the chromophores.[17] This can be understood as contributing to an increase in the number of available vibrational modes, leading to an enhanced rate of internal conversion. Orientational disorder in the solid state can presumably have a similar effect.

The results in Figure 5 and Table I show that increasing the order of the film leads to a large increase in the fluorescence efficiency. The least ordered ZnOEP film (curve 2, Figure 5) fluoresces ca. 25% as efficiently as the most ordered ZnOEP film (curve 3) and only ca. 5% as efficiently as the as-spun liquid crystal film (curve 4). This latter film has a quantum yield for fluorescence comparable to that of the solution species (curve 1, Figure 5). Because of differences in reflection effects and film thickness (ca. 100 μm for the solution, ca. 0.1 μm for the thin films), it is difficult to make an exact comparison of quantum yields. However, in the large number of films examined, an increase in fluorescence efficiency with increased order of the film (as seen by the blue-shift and narrowing of the B band) has always been observed. Thus, fluorescence quenching of thin films, at least in the case of octaalkylporphyrins, is not a necessary consequence of electronic coupling, but rather is a function of the disordered environment.

The fluorescence efficiency of the films always diminished upon heating; thus, it is difficult to compare the ordered (i.e., heated to ca. 170 °C and then cooled) liquid crystal, curve 5, to the film as-spun, curve 4 (Figure 5). Ordering ZnOOEP resulted in a decrease of 10–15% in Φ_f. This was independent of substrate or whether the film was heated under nitrogen or vacuum. The same heat treatment of ZnOEP caussed Φ_f to decrease by 40–60%. This is possibly the result of a reaction with an impurity. Thus, it is not yet clear whether the trend of increasing Φ_f with increasing order extends to film 5.

Indium tin oxide (ITO) is known to quench the fluorescence of porphyrins.[22] ITO substrates were used for reasons detailed in the Experimental Section and because our ultimate goal is to investigate the photoelectron transfer properties of these films. The fluorescence quenching is a strong function of porphyrin film thickness, and control experiments comparing microscope slide and ITO substrates show that this quenching is on the order of 5–15% for these spin-coated films. Therefore, the reported quantum yields for fluorescence of the thin films are probably low by this amount.

The cell with ZnOOEP crystallized from dodecane, samples 6 and 7, was prepared from a very dilute solution in order to make the sample optically thin, with approximately equal absorbances at the B bands of the dissolved and crystalline species (see Table I). Emission spectra taken with excitation at 404 (dissolved porphyrin) and 385 nm (crystalline porphyrin), followed by subtraction of the spectrum of the minor component, then gave a comparison of the emission quantum yields of the solution and the crystalline species, this time in the same cell with the same scattering and reflection effects. These data are also shown in Table I. The apparent Φ_f (see discussion of the excitation spectra below) of the crystalline species was equal to that of the solution species, providing further evidence that the fluorescence is not necessarily quenched in the solid relative to solution. The results with this cell also demonstrate that the photophysical properties of ordered porphyrin thin films are very similar to those of (free-floating) crystals. That is, the substrate and the spin-coating procedure do not introduce any noticeable artifacts into the measurements.

The Stokes shift for weakly coupled molecules in the solid state is related to the thermal relaxation of the neighboring molecules around an excited molecule, which, in turn, is a function of the orientation and the homogeneity of the neighbors. The Stokes shift (the difference between the Q(0, 0) absorption and emission peaks) in these films decreases with increasing order (Table I), except for the capillary-filled sample, curve 8, and tends toward the value for a solution species. Sample 8 shows an increased Stokes shift, possibly resulting from a greater delocalization of the excited state caused by stronger intermolecular coupling, as discussed below.

(26) Jortner, J.; Bixon, M. *Mol. Cryst. Liq. Cryst.* **1969**, *9*, 213.

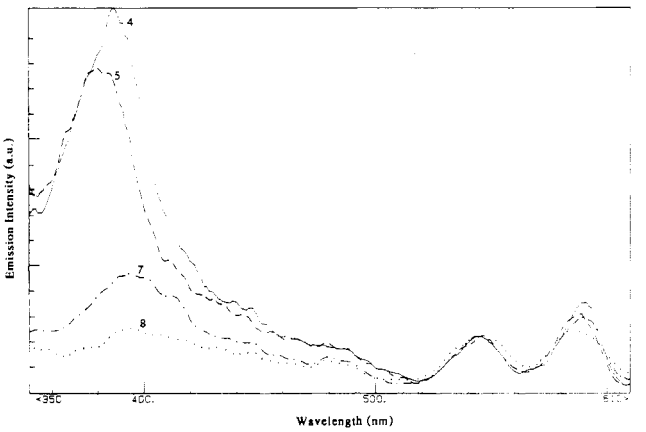

Figure 6. Excitation spectra. Emission monitored at 650 nm. Numbers correspond to the samples shown in Figures 3 and 4. Spectra are normalized at 545 nm.

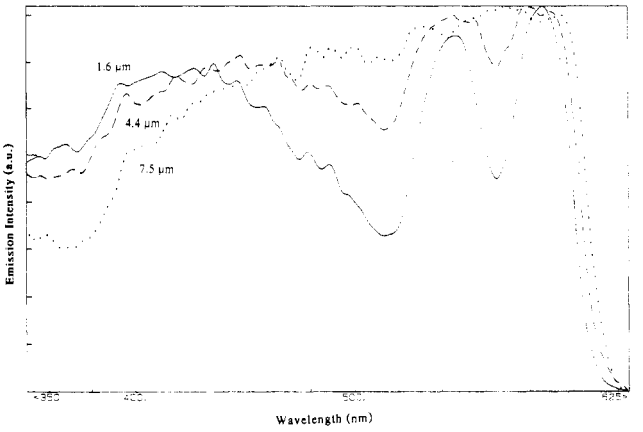

Figure 7. Excitation spectra as a function of thickness. Emission monitored at 650 nm. Spectra were taken from a single, capillary-filled wedge cell. The numbers give the approximate thickness (μm) of the cell at that point. Spectra are normalized at the highest point.

Excitation Spectra. In Figure 6 are shown the excitation spectra of ZnOOEP thin films, curves 4 and 5, of the crystallized compound, curve 7, and of the capillary-filled cell, curve 8. The excitation spectra of films 2 and 3 were similar to film 4. The emission was monitored at 650 nm to avoid inner-filter effects, and the spectra were normalized at the peak of the Q(1, 0) band. In solution, the excitation spectra of ZnOOEP (not shown) match the absorption spectrum (normalized by the use of eq 3). This is also true, within experimental error (ca. ±15%), for the spin-coated thin films (samples 2–5). This shows that, in the thin films, as in solution, the quantum yield for internal conversion from S_2 (B band) to S_1 (Q bands) is unity. However, the most highly ordered porphyrins, samples 7 and 8, show strongly quenched emission when excited near the B band. The B band is quenched by a factor of 1.5 ± 0.2 in sample 7 and by a factor of 1.7 ± 0.3 in sample 8. To minimize scattering, it was necessary to excite the samples near the B band in our emission studies. Therefore, to calculate the relative quantum yield for emission of sample 7, we multiplied the integrated intensity by the factor 1.5 ± 0.2. We believe that this procedure, together with the fact that all spectra were measured in the same geometry, eliminates most of the error associated with a quantitative comparison of these various fluorescence spectra.

The quenching of fluorescence upon B band excitation was investigated as a function of increasing film thickness (Figure 7). These spectra were taken from a single, wedge-shaped, capillary-filled cell whose thickness varied from 1 to ca. 8 μm. The cell was positioned so that individual 2-mm-wide segments could be sequentially illuminated. At its thickest point, the porphyrin absorbs practically all of the incident light from 350 to 600 nm.

Under these conditions, its excitation spectrum is directly proportional to a plot of Φ_f vs λ,[24] assuming that the collection efficiency of the emitted photons is independent of wavelength. This assumption was tested by measuring excitation spectra at angles of incidence varying from 35° to 70° to the sample surface. To minimize scattering and reflection, excitation spectra were also measured in an in-line geometry, in which the excitation is incident on the back sample surface at 90° and emission is monitored at 90° to the front sample surface. The trend shown in Figure 7 was reproduced in all of these experiments. Hence, we conclude the Φ_f increases with increasing wavelength. That is, the fluorescence efficiency decreases with increasing energy of the exciting light for the most highly crystalline samples. Similar results have been reported for pyrene single crystals.[27]

There are several possible explanations of this effect: (1) It is caused by preferential reflection or scattering of light of shorter wavelength, leading to a decrease in excitation intensity with increasing energy. This is unlikely given the lack of a dependence on the angle of excitation. Nor would reflection losses alone explain the clear dependence on the crystallinity of the sample (Figure 6). (2) It is caused by exciton–exciton quenching[3] due to a high concentration of excitons created when exciting at a wavelength of high absorptivity. However, variation of the incident intensity over 2 orders of magnitude led to no change in the excitation spectra. Also, the B band is quenched relative to the Q bands even at wavelengths where their absorptivities are equal. This last fact also makes an exciton–surface quenching mechanism unlikely. (3) Exciton splitting produces a lower lying, optically forbidden, singlet state (B^-) that quenches the B^+ emission. (This is commonly seen in blue-shifted dimer and trimer systems.[21b,e]) However, in our case, a singlet state lying between the allowed S_2 and S_1 states would probably increase the rate of internal conversion to S_1 (the energy gap law), resulting in equal or increased emission from S_1. If the exciton splitting were large enough to cause B^- to be lower in energy than Q(0, 0), the fluorescence from both B and Q band excitation would be quenched, contrary to observation. (4) Electron-hole pair formation, with subsequent radiationless recombination, is competing with internal conversion to S_1. This would be consistent with the decrease in emission with increasing energy of excitation and with its dependence on increasing crystallinity of the sample. The energy difference between a separated cation radical and an anion radical of ZnOEP is ca. 2.1 eV in CH_2Cl_2.[28] This corresponds to light of $\lambda \approx 590$ nm. This value should represent an upper limit for the energy of a ring-to-ring charge-transfer (RRCT) state in a solid porphyrin because of the stabilizing coulombic attraction between the oppositely charged rings.[21d] The coupling between the excited singlet state manifold and states having charge-transfer character is expected to increase with increasing energy.[26,29] Geacintov et al.[27] correlated the decrease in Φ_f of pyrene crystals at shorter wavelength with the increasing conductivity caused by bulk generation of charge carriers. Whether the proposed RRCT state in ZnOOEP is formed by autoionization of a Frenkel exciton, as suggested for some systems,[27,29] or by direct charge-transfer excitation,[30] is not yet known. Thus, fluorescence quenching through RRCT-state formation is a possible explanation for the decrease in Φ_f with wavelength. This question and others related to electron transfer in these films will be the subject of a separate publication.[31]

Temperature Effects on Fluorescence Spectra. Figures 8 and 9 show the changes in the fluorescence emission and excitation spectra as a thin film of ZnOOEP changes phase from crystal (K) to liquid crystal (LC) (107 °C) and from LC to isotropic liquid (I) (162 °C). Figure 8 shows that the peak positions in the emission spectra at 88 °C are unchanged relative to those observed at 21 °C, but both peaks are broader, and the single

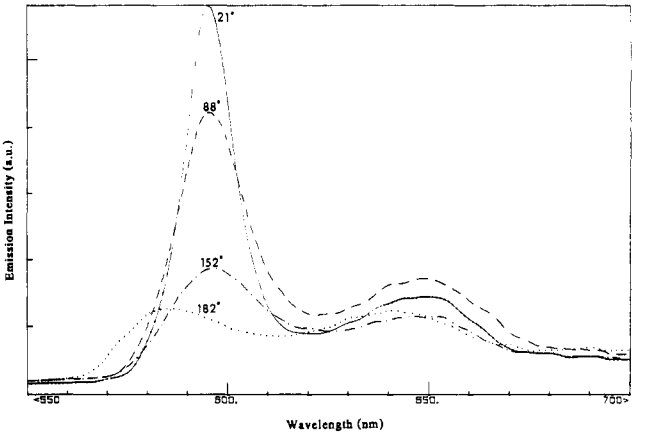

Figure 8. Emission spectra of an as-spun thin film of ZnOOEP as a function of temperature. Excitation wavelength was 390 nm. The phase transitions occur at 107 °C (crystal/liquid crystal) and 162 °C (liquid crystal/isotropic liquid).

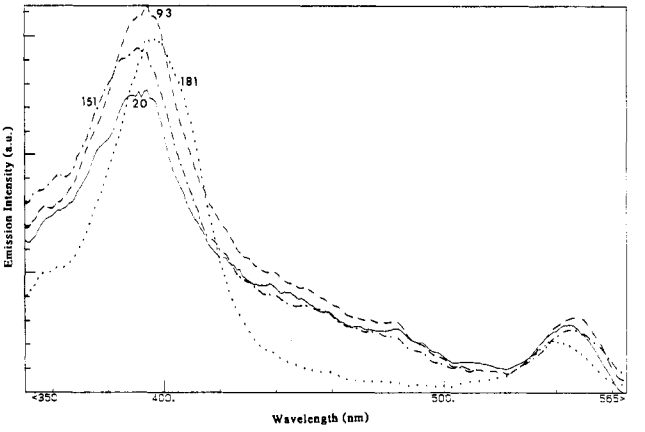

Figure 9. Excitation spectra of an as-spun thin film of ZnOOEP as a function of temperature. Emission was monitored at 650 nm. The phase transitions occur at 107 °C (crystal/liquid crystal) and 162 °C (liquid crystal/isotropic liquid).

phonon band, Q(0, 1) at 645 nm, has gained slightly in intensity relative to the Q(0, 0) band. No dramatic changes are observed at 152 °C in the LC phase, consistent with the relatively well-ordered structure of the film as spin-coated. A slight red-shift in the emission peaks (2 nm) suggests some increased order. Upon melting to the isotropic liquid, shown at 182 °C, both bands are blue-shifted by 11 nm relative to the LC phase, signifying a decrease in the order of the film and decreased exciton coupling.

The corresponding excitation spectra, done on a similar film, are shown in Figure 9. The signal is increased at 93 °C relative to 20 °C due to the increase in emission from Q(0, 1) seen in Figure 8. Again, the spectrum (151 °C) is not changed markedly on going to the liquid crystalline phase; the B band is blue-shifted by 4 nm relative to its position at 93 °C. After the sample was melted to the isotropic liquid, the spectrum (181 °C) shows a sharper B band than in the LC phase and its intensity has increased relative to the Q(1, 0). The B band has been red-shifted by 7 nm and the Q(1, 0) blue-shifted by 7 nm relative to the LC phase. Most noticeable is the complete disappearance of the low-energy tail on the B band and of the two peaks around 448 and 486 nm.

The absorption spectra have also been measured as a function of temperature (not shown); they are essentially identical with the excitation spectra (Figure 9). In particular, the long-wavelength tail on the B band and the bands at ca. 448 and 486 nm disappear upon melting to the isotropic liquid and reappear upon cooling back into the liquid crystalline phase.

The excitation, emission, and absorption spectra of ZnOOEP in the liquid phase more closely resemble those of the monomer in solution than those of the solid. These spectra demonstrate clearly that the spectral shifts seen in these materials are not caused merely by the proximity of the neighboring chromophores but

(27) Geacintov, N.; Pope, M.; Kallman, H. *J. Chem. Phys.* **1966**, *45*, 2639.
(28) Davis, D. G. In Reference 13, Vol. 5.
(29) Chance, R. R.; Braun, C. L. *J. Chem. Phys.* **1976**, *64*, 3573.
(30) (a) Bounds, P. J.; Siebrand, W. *Chem. Phys. Lett.* **1980**, *75*, 414. (b) Bounds, P. J.; Siebrand, W. *Chem. Phys. Lett.* **1982**, *85*, 496.
(31) Gregg, B. A.; Fox, M. A.; Bard, A. J., manuscript in preparation.

rather by the specific organization of the neighbors.

The spectral shifts shown in Figures 8 and 9, and those of the absorption spectra, are qualitatively reversible. As previously mentioned, heating the porphyrin causes a decrease in Φ_f, and heating to the isotropic liquid phase causes some coalescence of the films. Furthermore, after cooling, the porphyrin is more ordered, with its attendant spectral shifts, than upon first warming.

Conclusions

Increasing the order of zinc octaalkylporphyrin thin films leads to characteristic changes in the absorption spectra that, for all but the most highly ordered films, can be explained on the basis of the molecular exciton model. The fluorescence quenching commonly seen in porphyrin thin films relative to the monomer in solution is shown to be a result of disorder. In ordered films, the fluorescence quantum yield, Φ_f, becomes comparable to the Φ_f in solution. In the most highly crystalline sample (the capillary-filled cell), the B band is broadened, the Q(0, 0) band is weakened and blue-shifted, and the Stokes shift is increased relative to the most ordered spin-coated film. Thus, several trends seen upon ordering of the spin-coated thin films are reversed. This reversal coincides with the appearance of a wavelength-dependent fluorescence quantum yield that decreases with increasing energy of excitation. This suggests that ring-to-ring charge-transfer-state formation may compete with fluorescence in the most highly crystalline samples. The photophysical properties of the pure liquid porphyrins show that the spectral shifts seen in these thin films are a function of the organization, not merely the proximity, of the neighboring chromophores.

Acknowledgment. We are grateful to the National Science Foundation for support of the Materials Research Group at the University of Texas under whose aegis this work was performed. We also thank Professor Steven E. Webber for his helpful comments on the manuscript.

Registry No. ZnOOEP, 119567-75-8; ZnOEP, 17632-18-7.

Pronounced Pressure Effects on Reversible Electrode Reactions in Supercritical Water

William M. Flarsheim,[†] Allen J. Bard,[‡] and Keith P. Johnston*,[†]

Departments of Chemical Engineering and Chemistry, The University of Texas, Austin, Texas 78712
(Received: August 22, 1988)

An alumina electrochemical cell containing an ultramicroelectrode was used to make precise voltammetric measurements in supercritical water. The effect of pressure on the redox potential of the I_2/I^- couple was measured from 230 to 300 bar at 385 °C. The partial molar volume change for the reduction of I_2 to I^-, $\Delta\bar{v}_{rxn}$, is pronounced, mostly because of the interplay between strong electrostatic forces and the large isothermal compressibility of the fluid. A modified Born model together with a perturbed hard sphere equation of state predicts the data accurately above 265 bar with no adjustable parameters. At lower pressures, ion pairing is thought to reduce the magnitude of $\Delta\bar{v}_{rxn}$. These large pressure effects on solvation free energies may be used to manipulate reaction equilibria and reaction mechanisms in supercritical water.

Introduction

A unique and useful feature of a supercritical fluid solvent is the pronounced effect of pressure on density and density-dependent properties such as the chemical potential of a solute. For example, the partial molar volume, that is $\partial\mu_i/\partial P$, of naphthalene at infinite dilution in supercritical ethylene is thousands of cm^3/mol negative because of the large compressibility of the solvent.[1] Partial molar volumes would be expected to be even more extreme in water due to the much larger change in the dielectric constant with pressure, and in the case of an ionic solute, to the strength of electrostatic forces. The objective of this work is to measure partial molar volume changes of reaction ($\Delta\bar{v}_{rxn}$) in supercritical water and to analyze the data theoretically in terms of pressure effects on solvation free energies and structures. The effects of both the ionic and nonionic intermolecular interactions will be analyzed independently to provide a fundamental understanding of solvation in expanded water. This is the first study to explore quantitatively the effect of pressure on redox potentials in supercritical water. A comparison between theory and experiment will be used to explain large pressure effects on reversible electrode reactions.

Previously, we performed electrochemical techniques such as voltammetry and chronoamperometry in supercritical water at extreme temperatures and pressures up to 400 K and 240 bar, respectively.[2] Electrochemical potentials and kinetic parameters for redox reactions of both inorganic and organic species were investigated from room temperature up to 400 K at a given pressure of 240 bar. The measured diffusion coefficients of iodide ion and hydroquinone were described quantitatively by the Stokes–Einstein theory. Several other recent studies have considered the use of near-critical and supercritical fluid solvents as a medium to manipulate electrochemical reactions.[3-5]

Thermodynamic data on electrolytes, and solutes in general, in near-critical and supercritical water (T_c = 373.9 °C; P_c = 220.5 bar; v_c = 324.4 kg/m^3) are important for a number of scientific and industrial areas including mineral geology and the formation of ore deposits, corrosion and scaling in electric power boilers, oxidation of waste in supercritical water, hydrothermal materials processing, and processes for coal and oil upgrading. Early measurements in supercritical water were primarily of the vapor pressures and phase compositions of electrolyte solutions.[6,7] Current investigations include electrochemical studies of metal corrosion,[8-10] measurement of ionic conductances,[11,12] and the

[†] Department of Chemical Engineering.
[‡] Department of Chemistry.

(1) Eckert, C. A.; Ziger, D. H.; Johnston, K. P.; Kim, S. *J. Phys. Chem.* **1986**, *90*, 2738.
(2) Flarsheim, W. M.; Tsou, Y.; Trachtenberg, I.; Johnston, K. P.; Bard, A. J. *J. Phys. Chem.* **1986**, *90*, 3857.
(3) Crooks, R. M. Ph.D. Dissertation, University of Texas at Austin, 1987.
(4) Flarsheim, W. M.; Johnston, K. P.; Bard, A. J. *J. Electrochem. Soc.* **1988**, *135*, 1939.
(5) Dombro, R. A.; Prentice, G. A.; McHugh, M. A. *J. Electrochem. Soc.* **1988**, *135*, 2219.
(6) Keevil, N. B. *J. Am. Chem. Soc.* 1942, *64*, 841.
(7) Sourirajan, S.; Kennedy, G. C. *Am. J. Sci.* **1962**, *260*, 115.
(8) Macdonald, D. D. The Electrochemistry of Metals in Aqueous Systems at Elevated Temperatures. In *Modern Aspects of Electrochemistry, Vol. 11*; Bockris, J. O'M., Conway, B. E., Eds.; Plenum Press: New York, 1975; Chapter 4.
(9) Macdonald, D. D. *Corrosion* **1978**, *34*, 75.
(10) Macdonald, D. D.; Scott, A. C.; Wentreck, P. *J. Electrochem. Soc.* **1981**, *128*, 250.
(11) Marshall, W. L. *Pure Appl. Chem.* **1985**, *57*, 283.

0022-3654/89/2093-4234$01.50/0